An observational study of the effects of aerosols on diurnal variation of heavy rainfall and the concurrent cloud changes over Beijing-Tianjin-Hebei

Siyuan Zhou[1], Jing Yang[1,2*], Wei-Chyung Wang[3], Chuanfeng Zhao[2,4], Daoyi Gong[1,2], Peijun Shi[1,2]

[1] Academy of Disaster Reduction and Emergency Management, Faculty of Geographical Science, Beijing Normal University, China

[2] State Key Laboratory of Earth Surface Process and Resource Ecology, Beijing Normal University, China

[3]Atmospheric Sciences Research Center, State University of New York, Albany, New York 12203, USA

[4] College of Global Change and Earth System Science, Beijing Normal University, China

Submitted to ACP

Oct 2018

*Correspondence to: Jing Yang, State Key Laboratory of Earth Surface Process and Resource Ecology/Academy of Disaster Reduction and Emergency Management, Faculty of Geographical Science, Beijing Normal University, 19#Xinjiekouwai Street, Haidian District, Beijing 100875, China. E-mail: yangjing@bnu.edu.cn

Abstract: Our recent observational study found that the rainfall diurnal variation over Beijing-Tianjin-Hebei shows distinct signature of the effects of pollutants. Here we used the hourly rainfall measurements together with daily satellite-based information of aerosols and clouds to further study the responses of heavy rainfall and cloud properties to increases of pollutants. While the aerosol optical depth (AOD) and cloud droplet number concentration (CDNC) are both used as pollution indicators to provide a different perspective in rainfall study, CDNC is used exclusively on cloud changes. It is found that both indicators yield three consistent and distinguished responses of heavy rainfall: earlier start time, earlier peak time, and longer duration. However, quantitative differences exist between the two: for the first two responses, the advances are 0.7 and 1.0 hours respectively with AOD, but 2.1 and 4.2 hours respectively with CDNC; the third is prolonged by 0.8 hours with AOD and 2.4 hours with CDNC. In-depth analysis suggests that earlier in both start time and peak time occur in the presence of absorbing aerosols while the longer duration is attributed to scattering aerosols. Changes in cloud statistics caused by aerosols show increases in cloud fraction (11.1%), cloud top pressure (37.8 hPa), the liquid/ice cloud optical thickness (32.2/26.0) and cloud water path (239.8/422.0 g/m^2); and decreases in liquid/ice cloud effective radius (8.6/8.7μm). Analyses also indicate that increased moisture tends to decrease the cloud top pressure and enlarge the liquid cloud effective radius, which partially compensate the aerosol effects. Finally, the mechanisms accounted for the aerosol effects on heavy rainfall are hypothesized.

Key words: aerosol, heavy rainfall, diurnal variation, cloud, Beijing-Tianjin-Hebei, observational study

1. Introduction

Aerosols modify the global hydrologic cycle through both radiative effect (direct effect) and cloud effect (indirect effect) (IPCC, 2013). On the one hand, through absorbing or scattering solar radiation, aerosols can lead to the air aloft heating (e.g. Jacobson 2001; Lau et al. 2006) or the surface cooling (Lelieveld and Heintzenberg 1992; Guo et al. 2013; Yang et al., 2018), which changes the atmospheric vertical static stability and modulates rainfall (e.g. Rosenfeld et al. 2008). On the other hand, water-soluble aerosols serving as cloud condensation nuclei (CCN) could affect the warm-rain processes and cold-rain processes through influencing the cloud droplet size distributions, cloud top heights and other cloud properties (Jiang et al., 2002; Givati and Rosenfeld 2004; Chen et al., 2011; Lim and Hong 2012; Tao et al., 2012). Beijing-Tianjin-Hebei (BTH) region is the heaviest aerosol polluted area in China and concerns have been raised about the aerosol-radiation-cloud-precipitation interaction over this region. The impact of aerosols on light rainfall or warm-rain processes over BTH region almost reaches consistent agreement (e.g., Qian et al., 2009), but aerosol effects on the heavy convective rainfall in this region still have large uncertainties (Wang et al., 2009; Guo et al., 2014; Wang et al., 2016).

The clouds that can generate heavy convective rainfall in BTH region usually contain warm clouds, cold clouds and mixed-phase clouds (e.g. Guo et al., 2015). Because the aerosol-cloud interactions in different types of clouds are distinct (Gryspeerdt et al., 2014), aerosol indirect effect during heavy rainfall is more complicated than its direct effect (Sassen et al., 1995; Sherwood, 2002; Jiang et al., 2008, Tao et al., 2012). For warm clouds, by serving as CCN for more cloud droplets, aerosols can increase cloud albedo so called albedo effect or Twomey effect (Twomey, 1977), lengthen the cloud lifetime so called lifetime effect (Albrecht, 1989), and enhance thin cloud thermal emissivity so called thermal emissivity effect (Garrett and Zhao, 2006). The above effects tend to increase the cloud microphysical stability and suppress warm-rain processes (Albrecht 1989; Rosenfeld et al. 2014). For cold clouds and mixed-phase clouds, many studies reported that the cloud liquid accumulated by aerosols is converted to ice hydrometeors above the freezing level, which invigorates deep convective clouds and intensifies heavy precipitation so called invigoration effect (Rosenfeld and Woodley, 2000; Rosenfeld et al., 2008; Lee et al. 2009; Guo et al. 2014). The Twomey effect infers that aerosols serving as CCN increasing the cloud droplets could reduce cloud droplet size within a constant liquid water path (Twomey, 1977). However, the opposite results of relationship between aerosols and cloud droplet effective radius were reported in observations (Yuan et al., 2008; Panicker et al., 2010; Jung et al., 2013; Harikishan et al., 2016; Qiu et al., 2017), which might be related with the moisture supply near the cloud base (Yuan et al., 2008; Qiu et al., 2017). Besides, the influence of aerosols on ice clouds also depends upon the amount of moisture supply (Jiang et al., 2008). Therefore, how the aerosols modify the clouds associated with heavy convective rainfall does not reach a consensus, particularly if considering the different moisture conditions.

Heavy convective rainfall over BTH region usually occurs within a few hours, thus studying on the relationship between aerosols and rainfall diurnal variation could deepen our understanding of aerosol effects on heavy rainfall. Several previous studies have found that aerosols are related to the changes of the rainfall diurnal variation in other regions (Kim et al., 2010; Gryspeerdt et al., 2014; Fan et al., 2015; Guo et al., 2016; Lee et al., 2016). However, the above studies do not address the change of cloud properties and its sensitivity to different conditions of moisture supply. Although our recent work over BTH region (Zhou et al. 2018) attempted to remove the meteorological effect including circulation and moisture and found that the peak of heavy rainfall shifts earlier on the polluted condition, it only excluded the extreme moisture conditions and focused on aerosol radiative effect on the rainfall diurnal variation. Therefore, this study aims to deepen the previous study (Zhou et al., 2018) through investigating the following questions: (1) how do aerosols modify the different features of the diurnal variation of heavy rainfall (start time, peak time, duration and intensity)? (2) how do different types of aerosols (absorbing aerosols and scattering aerosols) modify the characteristics of heavy rainfall? (3) how do aerosols influence the concurrent cloud properties with inclusion of moisture? To solve above questions, we used aerosol optical depth (AOD) as an indicator of pollution to compare the characteristics of heavy rainfall, used cloud droplet number concentration (CDNC) representing CCN to investigate the changes of rainfall and clouds, and used aerosol index (AI) to distinguish the different effects of absorbing aerosols and scattering aerosols. The paper is organized as following: The data and methodology are introduced in Sect. 2. Section 3 presents the distinct characteristics of rainfall diurnal variation on clean/polluted conditions using AOD and CDNC. Section 4 addresses the impacts of different types of aerosols on characteristics of heavy rainfall. Section 5 describes the changes of cloud properties with the increase of CCN and moisture. Section 6 discusses the aerosol effects on cloud with inclusion of moisture, the distinct roles of aerosol radiative effect and cloud effect in heavy rainfall and the uncertainties of different indicators. Conclusion will be given in Sect. 7.

2. Data and methodology

2.1 Data

Four types of datasets from the year 2002 to 2012 (11 years) were used in this study, which include (1) precipitation, (2) aerosols, (3) clouds, and (4) other meteorological fields.

2.1.1 Precipitation data

To study the diurnal variation of heavy rainfall, the gauge-based hourly precipitation datasets were used, which were obtained from the National Meteorological Information Center (NMIC) of the China Meteorological Administration (CMA) (Yu et al., 2007) at 2420 stations in China from 1951 to 2012. The quality control made by CMA/NMIC includes the check for extreme values (the value exceeding the monthly maximum in daily precipitation was rejected), the internal consistency check (wiping off the erroneous records caused by incorrect units, reading, or coding) and spatial consistency check (comparing the time series of hourly precipitation with nearby stations) [Shen et al., 2010]. Here we chose 176 stations in the plain area of BTH region that are below the topography of 100 meter above sea level as shown in Fig.1, which is consistent with our previous work because we purposely removed the probable orographic influence on the rainfall diurnal variation (Zhou et al., 2018). The record analyzed here is the period of 2002 to 2012.

2.1.2 Aerosol data

AOD is a proxy for the optical amount of aerosol particles in a column of the atmosphere and serves as one of indicators for the division of aerosol pollution condition in this study, was obtained from MODIS (Moderate Resolution Imaging Spectroradiometer) Collection 6 L3 aerosol product with the horizontal resolution of 1°x1° onboard the Terra satellite (Tao et al., 2015). The quality assurance of marginal or higher confidence was used in this study. The reported uncertainty in MODIS AOD data is on the order of (-0.02-10%), (+0.04+10%) (Levy et al., 2013). The Terra satellite overpass time at the equator is around 10:30 local solar time in the daytime, which is before the occurrence of heavy rainfall events in this study as shown in Fig. 2. Therefore, the AOD used here represents the situation of the air quality in advance of heavy rainfall appearance.

The ultraviolet AI from Ozone Monitoring Instrument (OMI) on board the Aura satellite which was launched in July 2004 is used for detecting the different types of aerosols in this study. The OMI ultraviolet

AI is a method of detecting absorbing aerosols from satellite measurements in the near-ultraviolet wavelength region (Torres et al., 1998). The positive values of ultraviolet AI are attributed to the absorbing aerosols such as smoke and dust while the negative values of AI stand for the non-absorbing aerosols (scattering aerosols) such as sulfate and sea salt (Tariq and Ali, 2015). The near-zero values of AI occur when clouds and Rayleigh scattering dominate (Hammer et al., 2018). The horizontal resolution of AI data is 1°×1° and it covers the period of 2005 to 2012.

MACC-II (Monitoring Atmospheric Composition and Climate Interim Implementation) reanalysis product produced by ECMWF (the European Centre for Medium-Range Weather Forecasts), provided the AOD datasets for different kinds of aerosols (BC, sulfate, organic matter, mineral dust and sea salt). MACC-II reanalysis products are observationally-based within a model framework, which can offer a more complete temporal and spatial coverage than observation and reduce the shortcomings of simulation that fail in simulating the complexity of real aerosol distributions (Benedetti *et al*., 2009). The horizontal resolution of MACC-II is also 1°×1° with the time interval of six-hour. MACC-II data covers the period of 2003 to 2012.

2.1.3 Cloud data

Daily cloud variables, including cloud fraction (CF), cloud top pressure (CTP), cloud optical thickness (COT, liquid and ice), cloud water path (CWP, liquid and ice) and cloud effective radius (CER, liquid and ice), were obtained from MODIS Collection 6 L3 cloud product onboard the Terra satellite. The MODIS cloud product combines infrared emission and solar reflectance techniques to determine both physical and radiative cloud properties (Platnick et al., 2017). The validation of cloud top properties in this product has been conducted through comparisons with CALIOP (Cloud-Aerosol Lidar with Orthogonal Polarization) data and other lidar observations (Holz et al., 2008; Menzel et al., 2008), and the validation and quality control of cloud optical products is performed primarily using in situ measurements obtained during field campaigns as well as the MODIS Airborne Simulator instrument (https://modis-atmos.gsfc.nasa.gov/products/cloud). Since the clouds associated with heavy rainfall in the BTH region during early summer contain warm clouds, cold clouds and mixed-phase clouds (e.g. Guo et al., 2015), we purposely selected the clouds with its top pressure above 600 hPa to investigate both liquid and ice cloud properties because the 0°C isotherm of BTH region is nearly located at this height. Consistent with AOD, the measure of above cloud variables is before the occurrence of heavy rainfall.

CDNC is retrieved as the proxy for CCN and also another indicator for separating different aerosol conditions in this study. Currently, most derivations of CDNC assume that the clouds are adiabatic and horizontally homogeneous; CDNC is constant throughout the cloud's vertical extent, and cloud liquid water content varies linearly with altitude adiabatically (Min et al., 2012; Bennartz and Rausch, 2017). According to Boers et al. (2006) and Bennartz (2007), we calculated CDNC (unit: cm^{-3}) through:

$$\mathrm{CDNC} = \frac{{C_W}^{1/2}}{k}\frac{10^{1/2}}{4\pi{\rho_w}^{1/2}}\frac{\tau^{1/2}}{{R_e}^{5/2}} \quad (1)$$

Where C_w is the moist adiabatic condensate coefficient, and its value depends slightly on the temperature of the cloud layer, ranging from 1 to 2. 5 x 10^{-3} gm^{-4} for a temperature between 0 ℃ and 40 ℃ (Brenguier, 1991). In this study, we calculated the C_w through the function of the temperature (see Fig.1 in Zhu et al., 2018) at a given pressure that is 850 hPa. And we have tested the sensitivity of CDNC to the amount of C_w and found it almost keeps the same when the C_w changes from 1 to 2. 5 x 10^{-3} gm^{-4}. The coefficient k is the ratio between the volume mean radius and the effective radius and varies between 0.5 and 1 (Brenguier et al., 2000). Here we used k = 1 for that we cannot get the accurate value of k and the value of k does not influence the rank of CDNC for the division of aerosol condition in this study. ρ_w is cloud water density. τ and Re are the COT and CER obtained from MODIS Collection 6 L3 cloud product onboard the Terra satellite.

2.1.4 Other meteorological data

Other meteorological factors, including wind, temperature, pressure and specific humidity, were obtained from the ERA-Interim reanalysis datasets with 1°x1 °horizontal resolution and 37 vertical levels at six-hour intervals. ERA-Interim is the global atmospheric reanalysis produced by ECMWF, which covers the period from 1979 to near-real time (Dee et al., 2011). The absolute humidity (AH), which stands for the water vapor content of air per unit volume, is calculated as the indicator of moisture supply in this study. We calculated the AH (unit: g/m^3) through:

$$\mathrm{AH} = \frac{1000e}{R_v T} \tag{2}$$

Where R_V is the specific gas constant, which is 461.5 J kg^{-1} K^{-1}. T is air temperature (unit: K), and the vapor pressure *e* (unit: hPa) is calculated by the equation below:

$$\mathrm{q} = \frac{0.622e}{P-(1-0.622)e} \tag{3}$$

Where q is specific humidity (unit: kg/kg) and P is atmosphere pressure (unit: hPa), which were both obtained from ERA-interim.

2.2 Methodology

2.2.1 Method of interpolation

We used both station data of gauge-based precipitation and gridded data including aerosols, clouds and other meteorological variables. Gridded datasets in this study were downloaded with the horizontal resolution of 1°×1°, which are consistent with the resolution of MODIS L3 product. To unify the datasets, we interpolated all the gridded datasets onto the selected 176 rainfall stations using the average value in a 1°×1° grid as the background condition of each rainfall station, i.e., the stations in the same 1°×1° grid have the same aerosol, cloud and meteorological conditions.

2.2.2 Selection of sub-season and circulation

Consistent with our previous work, we focused on early summer (1 June to 20 July) before the large-scale rainy season starts, in order to remove the large-scale circulation influence and identify the effect of aerosols on local convective precipitation because BTH rainfall during this period is mostly convective rainfall (Yu et al., 2007) with heavy pollution (Zhou et al., 2018). And to unify the background atmospheric circulation, we only selected the rainfall days with southwesterly flow, which is the dominant circulation accounting for 40% of total circulation patterns over the BTH region during early summer (Zhou et al., 2018).

2.2.3 Classification of the heavy rainfall, clean/polluted and moisture conditions

With the circulation of southwesterly, we selected heavy rainfall days when the hourly precipitation amount was more than 8.0 mm/hour (defined by *Atmospheric Sciences Thesaurus, 1994*). We used two indicators to distinguish the clean and polluted condition, which are AOD and CDNC. The 25^{th} and 75^{th} AOD/CDNC of the whole rainfall days are used as the thresholds of clean and pollution condition, and the values are shown in Tab.1. It shows that there are 514 cases of heavy rainfall on polluted days and 406 cases of that on clean days when using AOD, and 924/894 cases on polluted/clean condition when using CDNC.

The absorbing aerosols are detected using the positive values of AI that is named as absorbing aerosol index (AAI) here, and we can retrieve the scattering aerosol index (SAI) using the negative values of AI. AAI and SAI are also divided into two groups using the threshold of 25^{th}/75^{th} as shown in Tab.1. We used AAI/SAI more than 75^{th} as the extreme circumstances of absorbing aerosols and scattering aerosols to compare their impacts on heavy rainfall. The case numbers are 375 and 550 events respectively for the extreme AAI and SAI cases. Using the same method, we chose cases of more BC/sulfate when the AOD of BC/sulfate is larger than the 75^{th} AOD of itself in all rainy days, and cases of less BC/sulfate when that is less than the 25^{th} AOD of itself in the same condition. Accordingly, we selected 459 cases of more BC and 274 cases of less BC with heavy rainfall. Similarly, 361 cases of more sulfate and 419 cases of less sulfate with heavy rainfall were selected.

The AH at 850 hPa is used as the indicator of moisture supply. We chose wet cases when the AH on that rainy day is larger than 75^{th} percentile of the whole rainy days, and chose dry cases when AH on that day is less than the 25^{th} percentile of the whole rainy days (the thresholds are shown in Tab. 1).

2.2.4 Statistical analysis

We adopted the probability distribution function (PDF) to compare the features of heavy rainfall and cloud variables on different conditions of aerosols, through which we can understand the changes of rainfall/cloud properties more comprehensively. The numbers of bins we selected in the study have been all tested for better representing the PDF distribution. Student's t-test is used to examine the significance level of differences between the different groups of aerosol conditions.

3 Distinct characteristics of heavy rainfall diurnal variation associated with aerosol pollution

Our previous study (Zhou et al. 2018) has reported the distinct peak shifts of rainfall diurnal variation between clean and polluted days using the indicator of AOD over the BTH region during early summer. Similar with our previous study, the PDF of the heavy rainfall peak time shows that the maximum of rainfall peak is about two hours earlier on the polluted days (20:00 LST) than that on the clean days (22:00 LST) (Fig. 2a(2)). To comprehensively recognize the changes of rainfall diurnal variation associated with air qualities, here we examined the PDF of the start time, the duration and the intensity besides the peak time of heavy rainfall.

In terms of the start time of heavy rainfall, a significant advance is found as shown in Fig. 2a(1). The secondary peak on the early morning is ignored here because the early-morning rainfall might be associated with the mountain winds (Wolyn et al., 1994; Li et al., 2016) and the nighttime low-level jet (Higgins et al., 1997; Liu et al., 2012) that is beyond the scope of this study. The time for maximum frequency of heavy rainfall initiation is 6 hours earlier on the polluted days, shifting from around 0:00 LST on the clean days to the 18:00 LST. Regarding the rainfall durations, the average persistence of heavy rainfall on polluted days is 0.8 hours longer than that on clean days (Tab. 2). According to the PDF shown as in Fig. 2a (3), the occurrence of short-term precipitation (≤6 hours, Yuan et al., 2010) decreases while that of long-term precipitation (>6 hours, Yuan et al., 2010) increases. The intensity of hourly rainfall exhibits a decrease on the polluted days. However, compared with the other features, the change of intensity does not pass the 95% statistical confidence level.

The differences of rainfall characteristics between clean and polluted days above can be well detected using the indicator of AOD. Since this study would investigate the aerosol-cloud interaction, the property of aerosol serving as CCN should be emphasized. In this condition, we did the similar analysis to verify the results above using the retrieved CDNC as the indicator of CCN (Zeng et al., 2014; Zhu et al., 2018) since AOD is not a proper proxy for CCN (Shinozuka et al., 2015). As a result, the same phenomenon can be well exhibited as shown in Fig. 2b. The start time and peak time of the heavy rainfall on polluted condition also show significant advances compared with the clean condition, with the average advances of 2.1 hours and 4.2 hours respectively (Tab. 2). The duration of heavy rainfall on the polluted condition is also prolonged, which is 2.4 hours longer in average (Tab. 2). Similar with the results based on AOD, the difference of rainfall intensity between clean and polluted conditions using CDNC does not pass the 95% statistical confidence level as well.

Both results of AOD and CDNC show that the start and peak time of heavy rainfall occur earlier and the duration becomes longer under pollution, although the quantitative differences exist between the two indicators. Since the difference of rainfall intensity is not significant, the following study only focuses on investigating why the start time, peak time and duration of heavy rainfall change with pollution in the diurnal time scale.

4 Impacts of different aerosols on rainfall diurnal variation

Using the indicator of AI, we further investigate the different changes of rainfall characteristics related to absorbing aerosols and scattering aerosols respectively. The PDF of start time, peak time and duration of heavy rainfall under the extreme circumstances of absorbing aerosols and scattering aerosols are compared in Fig. 3. The rainfall start time on absorbing aerosol days shows a significant advance with the maximum frequency occurring at 20:00 LST, compared with the 3:00 LST on scattering aerosol days (Fig. 3a). Similarly, the rainfall peak time also shows earlier on absorbing aerosol days, with an average advance of 1.7 hours (Fig. 3b). The rainfall duration on scattering aerosol days shows longer than that on absorbing aerosol days, which are 5.9 hours and 5.0 hours respectively in average. All the differences above between the two groups have passed 95% statistical confidence level. The results indicate that the absorbing aerosols and scattering aerosols may have different or inverse effect on heavy rainfall that absorbing aerosols may generate the heavy rainfall in advance and the scattering aerosols may delay and prolong the heavy rainfall.

To further distinguish the effects of the absorbing/scattering aerosols on the heavy rainfall, we purposely re-examine the above findings through BC/sulfate that can represent typical absorbing/scattering aerosols over BTH region. BC has its maximum center over BTH region (Fig. 4a) and our previous study has indicated that the radiative effect of BC low-level warming may facilitate the convective rainfall generation (Zhou et al., 2018). The percentage of sulfate is also large in BTH region (Fig. 4b) and the sulfate is one of the most effective CCN that influences the precipitation in this region (Gunthe et al., 2011). Accordingly, we selected the cases with different amounts of BC and sulfate AOD to compare the role of them in the diurnal variation of heavy rainfall. The methods have been described in Sect. 2.2.3. The PDF of the start time, peak time and duration of heavy rainfall were shown for the higher and lower BC cases in Fig. 5a, respectively. The most striking result is that the maximum frequency of rainfall start time in high BC cases evidently shifts earlier by 7 hours from 19:00 LST to 2:00 LST. Meanwhile, compared with low BC cases, the mean peak time in high BC cases shows 1.0 hour earlier than that in low BC cases. And the duration of heavy rainfall is slightly shorter in high BC cases with the mean difference of 0.2 hours. These features of higher BC cases are consistent with the above absorbing aerosol effect. In contrast, when the sulfate has higher amount, the mean start time of rainfall is delayed by 0.5 hours, while the duration shows a significant increase by 1.5 hours in average. The behaviors of higher sulfate cases exhibit similar with the above scattering aerosol effect (Fig. 5b).

5 Cloud effect of aerosols with inclusion of moisture

5.1 Characteristics of clouds on clean and polluted condition based on CDNC

To understand the cloud effect of aerosols during heavy rainfall, we need to recognize the concurrent cloud characteristics on clean and polluted conditions. The cloud properties we used were obtained from satellite product which were measured at the same time as aerosols before the occurrence of heavy rainfall. The differences of cloud features were examined in both macroscopic properties (including CF, CTP, COT and CWP) and microscopic properties (including CER) between the clean and polluted condition based on CDNC, as shown in Fig. 6. The PDF distribution of CF shows that the CF on the polluted condition is evidently larger than that on the clean condition. The average CF is 82.5% on the clean condition and 93.6% on the polluted condition. The average CTP on the polluted condition is 436.0 hPa, more than that on the clean condition which is 398.2 hPa, indicating that the cloud top height is lower on the polluted days. According to PDF distribution, CTP on polluted condition has a significant peak at around 300 hPa and secondary maximum at around 550 hPa.

The COT, CWP and CER were further analyzed for the liquid and ice portions of clouds as shown in Fig. 6. Both liquid and ice COT on polluted condition exhibit a significant increase compared with that on clean condition. The mean amount of liquid COT increases by 32.2 and ice COT increases by 26.0. Similar with COT, the amount of liquid and ice CWP also increase on polluted condition. And the mean amount of liquid CWP increases by 239.8 g/m^2 and ice CWP increases by 422.9 g/m^2. The PDF of liquid CER on the polluted condition shows a shift to the smaller size and its mean value decreases by 8.6 μm. In accordance with the CER of liquid clouds, the CER of ice clouds also shows decrease with the mean difference of 8.7 μm. The differences of above cloud properties between clean and polluted cases have all passed the 95% statistical confidence level.

According to the above results, the increased CDNC corresponds to the increase of CF, COT, CWP for both liquid and ice clouds, but the decrease of cloud top height and CER (liquid and ice). Since we cannot distinguish the liquid part of mix-phased clouds from liquid (warm) clouds in the observation, the changes of liquid cloud properties above might come from both the liquid (warm) clouds and the liquid part of mixed-phase clouds. Likewise, the above-mentioned changes of ice cloud properties might come from both ice (cold) clouds and the ice part of mixed-phase clouds.

5.2 Influence of CCN and moisture on cloud properties

The different moisture supply under the cloud base can influence the cloud properties as well as the effect of aerosols on cloud properties (Yuan et al., 2008; Jiang et al., 2008; Jung et al., 2013; Qiu et al., 2017). It is hard to completely remove the moisture effect on the above results in a pure observational study. Since the southwesterly circulation cannot only transport pollutants but also moisture to the BTH region (Wu et al., 2017), more pollution usually corresponds to more moisture (Sun et al., 2015). Because the moisture supply for BTH is mainly transported via low-level southwesterly circulation, we purposely used the AH at 850 hPa as the indicator of moisture condition. To identify the effect of aerosols on clouds and its sensitivity to moisture, we purposely investigated the changes of above cloud properties with different conditions of CDNC and moisture respectively. We categorized all cases of heavy rainfall into four groups, which are (1) clean and dry, (2) polluted and dry, (3) clean and wet, (4) polluted and wet, and checked the changes of above cloud properties, as shown in Tab. 3. Here "clean/polluted" refers to the CDNC on that rainfall day less/more than $25^{th}/75^{th}$ percentile of the CDNC among the whole rainfall days, and similarly, the "dry/wet" refers to the AH on that rainfall day less/more than $25^{th}/75^{th}$ percentile of itself among the whole rainfall days. We made the significant test of differences between group 1 and 2, group 1 and 3, group 2 and 4, group 3 and 4.

Comparing the results of group 1 and 2, which are both on the dry condition, we can identify the influence of CDNC on cloud properties. The changes of these cloud variables are the same as that in Sect. 5.1, that the CF, COT and CWP both for liquid and ice are increased on the polluted condition, while the cloud top height and liquid and ice CER are decreased. Among these variables, the COT and CWP both for liquid and ice are especially larger on polluted condition, which are 2-5 times larger than that on clean condition. The liquid CER on polluted condition also changes evidently, which becomes almost a half of that on clean condition. On the wet condition, comparing the results of group 3 and 4, the changes are also similar that liquid and ice CER are decreased and others are increased except that the change of CTP is not significant. The results of the two comparisons above indicate that with the increase of CDNC (CCN), the CF, COT, CWP are increased while the CER is decreased regardless of the moisture amount.

Comparing the results of group 1 and 3, we can get the changes of cloud properties related only to moisture on the same clean condition. A common feature is that CF, cloud top height, COT and CWP both for liquid and ice clouds exhibit increases along with the increase of AH (the decrease of CTP corresponds to the increase of cloud top height). Compared with the CF on clean and dry condition (group 1), the increase of CF on clean and wet condition (group 3) is larger than that on polluted and dry condition (group 2), which indicates the influence of moisture on CF might be larger than the influence of CCN. In contrast with CF, the increases of COT and CWP both for liquid and ice clouds in group 2 are 2-3 times larger than that in group 3, which indicates that the influences of moisture on COT and CWP are evidently smaller than the influence of CCN. The influences of moisture on liquid and ice CER are not significant on the same clean condition. On polluted condition, comparing group 2 and 4, we found the same changes are the increase of CF, liquid COT and CWP, and the decrease of CTP, while the influences of moisture on ice COT and CWP on the polluted condition become not significant. When the moisture increases, the liquid CER on polluted condition is increased and the ice CER is decreased.

The results above indicate that both CCN and moisture have impacts on cloud properties. They both contribute to the increase of CF, COT and CWP, in which the influence of CCN on CF is smaller but its influences on COT and CWP are larger than moisture. The CCN and moisture have opposite effects on CTP, that the moisture can decrease the CTP which is lifting the cloud top, while CCN can lower the cloud top especially on the dry condition. The increase of CCN corresponds to the decrease of liquid and ice CER on the same dry/wet condition, but when the moisture increases, the liquid CER becomes slightly larger. While we should notice that the CDNC on dry or wet condition during heavy rainfall is naturally different, with the average value of 1614.2 cm^{-3} on dry condition and 2066.2 cm^{-3} on wet condition, which we cannot fix in an observation study. That is to say, when we divided the rainfall samples just by CDNC, the polluted condition with more CDNC actually stands for the situation of more CDNC and more moisture, and the clean condition represents the situation of less CDNC and less moisture. Thus, the results in Sect. 5.1 actually reflect the combined effect of CCN and moisture, which is consistent with the pure CCN effect mentioned above, indicating that the aerosol effect on these cloud properties is dominant on the polluted days.

6 Discussion

6.1 Possible effect of aerosols on cloud with inclusion of moisture

We attempt to understand the above results of aerosol effect on clouds with inclusion of moisture. The aerosols serving as CCN can nucleate a larger number of cloud droplets and accumulate more liquid water in the cloud, so the CF, COT and CWP become increased when the CCN increases or the moisture supply increases as in Tab 3. However, why the effects of CCN and moisture on cloud top height are opposite have not been clarified yet. Table 3 shows that the moisture could lift the cloud top height, which might due to the increase of cloud water that causes the non-precipitating clouds growing to be higher. While for the result of the lower cloud top height when CCN increases, we speculate it is because the precipitation process has started thus the clouds could not grow to be higher since the rainfall start time is advanced in Fig 2b.

The decrease of liquid CER caused by CDNC in the same dry/wet condition (Tab. 3) can be interpreted by Towmey effect that aerosols serving as CCN nucleate larger number concentrations of cloud drops, lead to the decrease of cloud droplet size for competing the cloud water within a constant liquid water path (Squires and Twomey, 1966; Twomey, 1977). When the moisture supply is more abundant, the liquid CER on the polluted condition (group 4 in Tab. 3) is relatively increased compared with drier condition (group 2 in Tab. 3). This might because the aerosols (CCN) increase the cloud droplet number, and the cloud water accordingly increases with increased moisture supply, thus the cloud drops potentially become larger via the adequate absorption of cloud water. We further investigate the relationship among CCN, CER and cloud water to verify above hypothesis, shown as in Fig. 7. That is, the liquid CER exhibits significantly decreased along with the increase of CDNC when fixing the cloud water. However, when increasing the cloud water, the liquid CER becomes larger at the same value of CDNC.

The study also has shown the ice CWP increases and the ice CER decreases under pollution, and the ice CER under pollution is still decreased when the moisture increases (Tab. 3). We assume the aerosols increase the cloud droplets so that reduce the vapor pressure inside clouds, thus decrease the supersaturation and weaken the process of transitions from liquid droplet into ice crystal, which is known as Bergeron process (Squires, 1952). Currently the detailed physical processes of cold clouds and mixed-phase clouds are not clear, including the diffusional grow, accretion, riming and melting process of ice precipitation (Cheng et al., 2010), which needs numerical model simulations to be further explored.

6.2 Different roles of aerosol radiative effect and cloud effect in heavy rainfall

In Sect. 3 we found that the heavy rainfall has earlier start time and peak time, and longer duration on the polluted condition. And afterwards, the earlier start of rainfall under pollution was found related to absorbing aerosols mainly referring to BC (Fig. 3a&5a). We also compared the effect of BC on the associated clouds. Figure 8a shows the CF larger than 90% rarely occurs in high BC environment, which might be associated with the semi-direct effect of BC (IPCC, 2013). This result indicates the influence of BC on the heavy rainfall in Fig. 5a is mainly due to the radiative effect rather than the cloud effect. The mechanism of BC effect on the heavy rainfall can be interpreted by our previous study (Zhou et al., 2018) as: BC absorbs shortwave radiation during the daytime and warms the lower troposphere at around 850 hPa, and then increases the instability of the lower to middle atmosphere (850-500hPa) so that enhances the local upward motion and moisture convergence. As a result, the BC-induced thermodynamic instability of the atmosphere triggers the occurrence of heavy rainfall in advance. Thus, the low-level heating effect of BC should play a dominant role in the beginning of rainfall especially before the formation of clouds during the daytime.

The delayed start of heavy rainfall with higher scattering aerosols in Fig. 2a and higher sulfate in Fig. 4b is consistent with many studies that both the radiative effect and cloud effect of sulfate-like aerosols could delay or suppress the occurrence of rainfall (Guo et al., 2013; Wang et al., 2016; Rosenfeld et al. 2014). Sulfate-like aerosols as scattering aerosols could prevent the shortwave radiation from arriving at the surface thus cool the surface and stabilize the atmosphere, which suppresses the rainfall formation (Guo et al., 2013; Wang et al., 2016). Sulfate-like aerosols serving as CCN can also suppress the rainfall by cloud effect through reducing the cloud droplet size and thus suppressing the collision-coalescence process of cloud droplets (Albrecht 1989; Rosenfeld et al. 2014). Figure 8b does shows that in contrast with BC, the CF larger than 90% is significantly increased in the high sulfate environment, which indicates the sulfate-like aerosols have evident influence on the clouds. We also verified that the cloud droplet shifts to a smaller size when the CDNC increases (Fig. 6) in Sect. 5, indicating that the cloud effect of aerosols could lead to the delay of the heavy rainfall occurrence. Another significant feature is the longer duration of heavy rainfall in the high scattering aerosol cases and high sulfate cases (Fig 3c&5b). We speculate that the longer duration is caused by the cloud effect of sulfate-like aerosols. When CCN increases over BTH region, the cloud droplet size is decreased but the cloud water is increased (Fig. 6). Therefore, the rainfall start time is delayed for the reduced collision-coalescence of cloud droplets, while the duration might be prolonged due to the significant increase of cloud water. To further investigate the mechanism of longer duration, we need the assistance of numerical model simulations in the future work.

Accordingly, we speculate that the earlier start time of heavy rainfall related to absorbing aerosols (BC) is due to the radiative heating effect of absorbing aerosols, while the longer rainfall duration associated with the scattering aerosols (sulfate) is mainly caused by the cloud effect of sulfate-like aerosols. As a summary using a schematic diagram (Fig. 9) to illustrate how aerosols modify the heavy rainfall over BTH region. On one hand, BC heats the lower troposphere, changing the thermodynamic condition of atmosphere, which increases upward motion and accelerates the formation of cloud and rainfall. On the other hand, the increased upward motion transports more sulfate-like particles into the clouds so that more CCN and sufficient moisture increase the cloud water, thus might prolong the duration of rainfall. As a result, the heavy rainfall shows earlier start and peak time, and longer duration due to the combined effect of aerosol radiative effect and cloud effect. To further distinguish the radiative effect and cloud effect of aerosols, we need to conduct numerical model simulations in our future study.

6.3 Uncertainties of different indicators

In this study, we used two indicators to discriminate the different pollution levels, which are AOD and CDNC. AOD is a good proxy for the large-scale pollution level, but it cannot well represent CCN (Shinozuka et al., 2015). The value of AOD is influenced by moisture condition (Twohy et al., 2009). CDNC is a better proxy for CCN, but it also has its uncertainties because it is calculated by the COT and CER. We can draw the same conclusion on heavy rainfall diurnal changes between clean and polluted condition when using AOD and CDNC respectively (Fig. 2). But when investigating the differences of cloud properties between clean and polluted condition, there is a different result between using AOD and using CDNC, that the liquid CER is decreased when CDNC increases (Fig. 6) while the liquid CER is increased when AOD increases. The difference might be related with that the measurement biases, e.g., satellite AOD is evidently influenced by the cloud (Brennan et al., 2005).

We applied ultraviolet AI and AOD of BC/sulfate to identify different types of aerosols. Ultraviolet AI in this study is only used to detect the extreme circumstances of absorbing aerosols and scattering aerosols since the near-zero values have larger uncertainties due to the cloud and other factors. The comparisons of BC/sulfate AOD cases also have uncertainties because they are retrieved from MACC reanalysis data. Although the four indicators all have their own uncertainties, we cannot find the more reliable datasets in a long-term observational record, and the major findings can be well shown in these four indices.

7. Conclusions

Using the gauge-based hourly rainfall records, aerosol and cloud satellite products and high temporal resolution reanalysis datasets during 2002-2012, this study investigated the different characteristics of heavy rainfall in the diurnal time scale on the clean and polluted conditions respectively. Based on two indicators that are AOD from MODIS aerosol product and retrieved CDNC from MODIS cloud product, we found three features of rainfall changing by aerosols that the rainfall start and peak time occur earlier and the duration becomes longer. The quantitative differences exist between the two indicators, i.e., the statistic differences of above features between clean and polluted conditions are 0.7, 1.0, 0.8 hours based on AOD and 2.1, 4.2, 2.4 hours based on CDNC. The different roles of absorbing aerosols and scattering aerosols in modifying the diurnal shift were also distinguishable using ultraviolet AI from OMI and reanalysis AOD of two aerosol types (BC and sulfate). The absorbing aerosols (BC) correspond to the earlier start time and peak time of heavy rainfall, while the scattering aerosols (sulfate) correspond to the delayed start time and the longer duration.

By comparing the characteristics of cloud macrophysics and microphysics variables, we found the CF, COT (liquid and ice), CWP (liquid and ice) are increased on the polluted condition based on CDNC, but the cloud top height and the CER (liquid and ice) are reduced. Considering moisture effect, the influence of aerosols on COT and CWP is relatively larger than the moisture effect, although both aerosols and moisture could increase the CF, COT and CWP. Liquid CER decreases almost a half under pollution, but when the moisture increases, it shows a slight increase compared with the dryer condition. The influences of aerosols and moisture on cloud top height are inverse, i.e., aerosols could lower the cloud top height while the moisture could lift the cloud top.

According to these results, we speculate that both aerosol radiative effect and cloud effect have impacts on the diurnal variation of heavy rainfall in BTH region. The heating effect of absorbing aerosols especially BC increases the instability of the lower to middle atmosphere so that generates the heavy rainfall occurrence in advance; and the increased aerosols nucleate more cloud droplets and accumulates more liquid water in clouds, the duration of heavy rainfall is accordingly prolonged.

This study has clearly identified the aerosol effect on diurnal changes of heavy rainfall and concurrent clouds in the BTH region and attempted to address the causes. However, although this work has attempted to exclude the impacts from the meteorological background particularly circulation and moisture, the observation study still has its limitation on studying aerosol effect on rainfall and cloud, such as the noise and uncertainty of different observational data, the interaction of aerosol and meteorological factors and the mixing of different types of aerosols. Numerical model simulations are necessarily applied to examine the speculation we proposed here. And the specific processes of aerosols effect on the mix-phased cloud precipitation formation also needs further exploration in our future study.

Data availability

We are grateful to the National Meteorological Information Centre (NMIC) of the China Meteorological Administration (CMA) for providing hourly precipitation datasets. MODIS aerosol and cloud data were obtained from http://ladsweb.modaps.eosdis.nasa.gov; ultraviolet AI data from OMI was obtained from https://daac.gsfc.nasa.gov/datasets?keywords=OMI&page=1; MACC-II and ERA-interim reanalysis datasets were obtained from http://apps.ecmwf.int/datasets.

Author contributions

JY and SZ conceived the study. SZ processed data and drew the figures. SZ and JY analyzed the observational results and WCW, CZ and DG gave the professional guidance. PS provided the hourly precipitation dataset. SZ and JY prepared the manuscript with contributions from WCW and CZ.

Competing interests

The authors declare that they have no conflict of interest.

Acknowledgements

This study is supported by funds from the National Key Research and Development Program-Global Change and Mitigation Project: Global Change Risk of Population and Economic System: Mechanism and Assessment (2016YFA0602401), the National Natural Science Foundation of China (grant nos. 41375003, 41621061 and 41575143) and Project supported by State Key Laboratory of Earth Surface Processes and Resource Ecology and Key Laboratory of Environmental Change and Natural Disaster. Wei-Chyung Wang acknowledges the support of a grant (to SUNYA) from the Office of Sciences (BER), U.S. DOE.

References:

Albrecht, B. A.: Aerosols, cloud microphysics, and fractional cloudiness, Science 245: 1227-1230, 1989.

Anonymous: 1994. Atmospheric Sciences Thesaurus. China Meteorological Press: Beijing, China. (in Chinese)

Anonymous (2013), IPCC fifth assessment report,Weather, 68, 310-310.

Bellouin, N., Quaas, J., Morcrette J. -J., and Boucher, O.: Estimates of aerosol radiative forcing from the MACC re-analysis. Atmos. Chem. Phys., 13: 2045-2062, 2013.

Benedetti, A., Morcrette, J. J., Boucher, O., Dethof, A., Engelen, R. J., Fisher, M., Flentje, H., Huneeus, N., Jones, L., Kaiser, J. W., Kinne, S., Mangold, A., Razinger, M., Simmons, A. J., and Suttie, M.: Aerosol analysis and forecast in the European Centre for Medium-Range Weather Forecasts Integrated Forecast System: 2. Data assimilation. J. Geophys. Res. 114: D13205 doi:10.1029/2008JD011115, 2009.

Brennan, J., Kaufman, Y., Koren, I., and Rong, L.: Aerosol-cloud interaction-Misclassification of MODIS clouds in heavy aerosol, IEEE T. Geosci. Remote, 43, 911–915, https://doi.org/10.1109/TGRS.2005.844662, 2005.

Bennartz, R., and Rausch, J.: Global and regional estimates of warm cloud droplet number concentration based on 13 years of AQUA-MODIS observations, Atmos. Chem. Phys., 17: 9815-9836, 2017.

Bennartz, R.: Global assessment of marine boundary later cloud droplet number concentration from satellite, J. Geophys. Res., 112, D02201, doi:10.1029/2006JD007547, 2007.

Boers, R., Acarreta, J. A., and Gras, J. L.: Satellite monitoring of the first indirect aerosol effect: Retrieval of the droplet concentration of water clouds, J. Geophys. Res., 111, D22208, doi:10.1029/2005JD006838, 2006.

Chen, Q., Yin, Y., Jin, L., Xiao, H., and Zhu, S.: The effect of aerosol layers on convective cloud microphysics and precipitation, Atmos. Res., **101,** 327-340, 2011.

Cheng, C. T., Wang, W. C., and Chen, J. P.: A modeling study of aerosol impacts on cloud microphysics and radiative properties, Q. J. R. Meteorol. Soc., 133, 283–297, doi:10.1002/qj.25, 2007.

Cheng, C. T., Wang, W. C., and Chen, J. P.: Simulation of the effects of increasing cloud condensation nuclei on mixed-phase clouds and precipitation of a front system. Atmos. Res., 96: 461-476, doi: 10.1016/j.atmosres.2010.02.005, 2010.

Dee, D. P., Uppala, S. M., Simmons, A. J., Berrisford, P., Poli, P., Kobayashi, S., Andrae, U., Balmaseda, M. A., Balsamo, G., Bauer, P., Bechtold, P., Beljaars, A. C. M., van de Berg, L,, Bidlot, J., Bormann, N., Delsol, C., Dragani, R., Fuentes, M., Geer, A. J., Haimberger, L., Healy, S. B., Hersbach, H., H´olm, E. V., Isaksen, L., K°allberg, P., K¨ohler, M., Matricardi, M., McNally, A. P., Monge-Sanz, B. M., Morcrette, J. –J., Park, B. –K., Peubey, C., de Rosnay, P., Tavolato, C., Th´epaut, J. –N., Vitart, F.: The ERA-Interim reanalysis: configuration and performance of the data assimilation system. Q. J. R. Meteorol. Soc. 137: 553–597. doi:10.1002/qj.828, 2011.

Fan, J. W., Rosenfeld, D., Yang, Y., Zhao, C., Leung, L. R., and Li, Z. Q.: Substantial contribution of anthropogenic air pollution to catastrophic floods in Southwest China. Geophys. Res. Lett. 42: 6066-6075, 2015.

Garrett, T. J. and Zhao, C.: Increased Arctic cloud longwave emissivity associated with pollution from mid-latitudes. Nature 440(7085): 787-9, 2006.

Givati, A., and Rosenfeld, D.: Quantifying precipitation suppression due to air pollution. J. Appl. Meteor. 43: 1038-1056, 2004.

Gryspeerdt, E., Stier, P., and Partridge, D. G.: Links between satellite-retrieved aerosol and precipitation. Atmos. Chem. Phys., 14, 9677–9694, 2014.

Gunthe, S. S., Rose, D., Su, H., Garland, R. M., Achtert, P., Nowak, A., Wiedensohler, A., Kuwata, M., Takegawa, N., Kondo, Y., Hu, M., Shao, M., Zhu, T., Andreae, M. O., and Poschl, U.: Cloud condensation nuclei (CCN) from fresh and aged air pollution in the megacity region of Beijing, Atmos. Chem. Phys. 11(21): 11023-11039, 2011.

Guo, C. W., Xiao, H., Yang, H. L., and Tang, Q.: Observation and modeling analyses of the macro-and microphysical characteristics of a heavy rain storm in Beijing, Atmos. Res., 156: 125-141, doi: 10.1016/j.atmosres.2015.01.007, 2015.

Guo, J. P., Deng, M. J., Lee, S. S., Wang, F., Li, Z. Q., Zhai, P. M., Liu, H., Lv, W., Yao, W., and Li, X. W.: Delaying precipitation and lightning by air pollution over the Pearl River Delta. Part I: Observational analyses. J. Geophys. Res. Atmos. 121: 6472-6488, 2016.

Guo, L., Highwood, E. J., Shaffrey, L. C., and Turner, A. G.: The effect of regional changes in anthropogenic aerosols on rainfall of the East Asian Summer Monsoon. Atmos. Chem. Phys. 13: 1521-1534, 2013.

Guo, X. L., Fu, D. H., Guo, X., and Zhang, C. M.: A case study of aerosol impacts on summer convective clouds and precipitation over northern China. Atmos. Res.142: 142-157, 2014.

Hammer, M. S., Martin, R. V., Li, C., Torres, O., Manning, M., and Boys, B. L.: Insight into global trends in aerosol composition from 2005 to 2015 inferred from the OMI Ultraviolet Aerosol Index, Atmos. Chem. Phys., 18: 8097-8112, 2018.

Harikishan, G., Padmakumari, B., Maheskumar, R. S., Pandithurai, G., and Min, Q. L.: Aerosol indirect effects from ground-based retrievals over the rain shadow region in Indian subcontinent, J. Geophys. Res. Atmos. 121(5): 2369-2382, 2016.

Higgins, R. W., Yao, Y., Yarosh, E. S., Janowiak, J. E. and Mo, K. C.: Influence of the Great Plains low-level jet on summertime precipitation and moisture transport over the central United States,J. Climate, 10, 481-507,1997.

Holz, R. E., Ackerman, S. A., Nagle, F. W., Frey, R., Dutcher, S., Kuehn, R. E., Vaughan, M. A., and Baum, B.: Global Moderate Resolution Imaging Spectroradiometer (MODIS) cloud detection and height evaluation using CALIOP, J. Geophys. Res. Atmos., 113: D00A19, doi: 10.1029/2008JD009837, 2008.

Jacobson, M. Z.: Strong radiative heating due to the mixing state of black carbon in atmospheric aerosols. Nature 409: 695-697, 2001.

Jiang, H., Feingold, G., and Cotton, W. R.: Simulations of aerosol-cloud-dynamical feedbacks resulting from entrainment of aerosol into the marine boundary layer during the Atlantic Stratocumulus Transition Experiment, J. Geophys. Res., 107(D24), 4813, doi:10.1029/2001JD001502, 2002.

Jiang, J. H., Su, H., Schoeberl, M. R., Massie, S. T., Colarco, P., Platnick, S., and Livesey, N. J.: Clean and polluted clouds: Relationships among pollution, ice clouds, and precipitation in South America, Geophys. Res. Lett., 35, L14804, doi: 10.1029/2008GL034631, 2008.

Jiang, M. J., Li, Z. Q., Wan, B. C., and Cribb, M.: Impact of aerosols on precipitation from deep convective clouds in eastern China. J. Geophys. Res. 121: 9607-9620, 2016.

Johnson, D. B.: The role of giant and ultra-giant aerosol particles in warm rain initiation, J. Atmos. Sci., 39, 448–460, doi:10.1175/1520-0469(1982)039<0448:TROGAU>2.0.CO;2, 1982.

Jung, W. S., Panicker, A. S., Lee, D. I., and Park, S. H.: Estimates of aerosol indirect effect from Terra MODIS over Republic of Korea, Advances in Meteorology, 2013 (976813): 1-8, http://dx.doi.org/10.1155/2013/976813, 2013.

Kim, K. –M., Lau, K. M., Sud, Y. C., and Walker, G. K.: Influence of aerosol radiative forcings on the diurnal and seasonal cycles of rainfall over West Africa and Eastern Atlantic Ocean using GCM simulation. Clim. Dyn. 35(1):115-126, doi: 10.1007/s00382-010-0750-1, 2010.

Lau, K. M., Kim, M. K., and Kim, K. M.: Asian summer monsoon anomalies induced by aerosol direct forcing: the role of the Tibetan Plateau. Clim. Dyn., 26: 855-864, 2006.

Lee, S. S., Donner, L. J., and Phillips, V. T. J.: Impacts of aerosol chemical composition on microphysics and precipitation in deep convection. Atmos. Res., 94, 220-237, 2009.

Lee, S. S., Guo, J., and Li, Z: Delaying precipitation by air pollution over the Pearl River Delta: 2. Model simulation. J. Geophys. Res. Atmos., 121: 11739-11760, 2016.

Lelieveld, J. and Heintzenberg, J.: Sulfate cooling effect on climate through in-cloud oxidation of anthropogenic SO2. Science 258: 117-120, 1992.

Levy, R. C., Mattoo, S., Munchak, L. A., Remer, L. A., Sayer, A. M., Patadia, F., and Hsu, N. C.: The Collection 6 MODIS aerosol products over land and ocean, Atmos. Meas. Tech., 6, 2989–3034, https://doi.org/10.5194/amt-6-2989-2013, 2013.

Li, H., Cui, X., Zhang, W., and Qiao, L.: Observational and dynamic downscaling analysis of a heavy rainfall event in Beijing, China during the 2008 Olympic Games,Atmos. Sci. Lett., 17, 368-376, 2016.

Li, Z., Niu, F., Fan, J., Liu, Y., Rosenfeld, D., and Ding, Y.: Long-term impacts of aerosols on the vertical development of clouds and precipitation, Nat. Geosci., 4, 888-894, 2011.

Lim, K. S. and Hong, S.: Investigation of aerosol indirect effects on simulated flash-flood heavy rainfall over Korea, Meteor. Atmos. Phys., **118,** 199-214, 2012.

Liu, G., Shao, H., Coakley Jr. J. A., Curry, J. A., Haggerty, J. A., and Tschudi, M. A.: Retrieval of cloud droplet size from visible and microwave radiometric measurements during INDOEX: Implication to aerosols' indirect radioactive effect, J. Geophys. Res., 108(D1), 4006, doi:10.1029/2001JD001395, 2003.

Liu, J., Wang, S., Zhang, W., and Wei, X.: Mechanism analysis of a strong convective weather in Hebei Province,Advances in Marine Science, 30, 9-16, 2012.

Menzel, W. P., Frey, R. A., Zhang, H., Wylie, D. P., Moeller, C. C., Holz, R. E., Maddux, B., Baum, B. A., Strabala, K. I., and Gumley, L. E.: MODIS global cloud-top pressure and amount estimation: Algorithm description and results, J. Appl. Meteorol. Clim., 47(4):1175-1198, doi: 10.1175/2007JAMC1705.1, 2008.

Min, Q., Joseph, E., Lin, Y., Min, L., Yin, B., Daum, P. H., Kleinman, L. I., Wang, J., and Lee, Y. –N.: Comparison of MODIS cloud microphysical properties with in-situ measurements over the Southeast Pacific, Atmos. Chem. Phys., 12: 11261-11273, 2012.

Panicker, A. S., Pandithurai, G., and Dipu, S.: Aerosol indirect effect during successive contrasting monsoon seasons over Indian subcontinent using MODIS data, Atmospheric environment 44(15): 1937-1943, 2010.

Platnick, S., Meyer, K., King, M. D., Wind, G., Amarasinghe, N., Marchant, B., Arnold, G. T., Zhang, Z., Hubanks, P. A., Holz, R. E., Yang, P., Ridgway, W. L., and Riedi, J.: The MODIS cloud optical and microphysical products: Collection 6 updates and examples from Terra and Aqua. IEEE Trans. Geosci. Remote Sens., 55, 502-525, doi:10.1109/TGRS.2016.2610522, 2017

Qian, Y., Gong, D. Y., Fan, J. W., Leung, L. R., Bennartz, R., Chen, D. L., Wang, W. G.: Heavy pollution suppresses light rain in China: Observations and modeling. J. Geophys. Res. Atmos. **114:** D00K02, 2009.

Qiu, Y., Zhao, C., Guo, J., and Li, J.: 8-Year ground-based observational analysis about the seasonal variation of the aerosol-cloud droplet effective radius relationship at SGP site. Atmos. Environ. 164: 139-146, 2017.

Rienecker, M. M., Suarez, M. J., Todling, R., Bacmeister, J., Takacs, L., Liu, H. C., Gu, W., Sienkiewicz, M., Koster, R. D., Gelaro, R., Stajner, I., Nielsen, J. E.: The GEOS-5 Data Assimilation System—Documentation of Versions 5.0.1 and 5.1.0, and 5.2.0. NASA Technical Report Series on Global Modeling and Data Assimilation NASA/TM-2008 -104606 27: 92 pp, 2008.

Rosenfeld, D.: TRMM observed first direct evidence of smoke from forest fires inhibiting rainfall, Geophys. Res. Lett., 26, 3105–3108, doi:10.1029/1999GL006066, 1999.

Rosenfeld, D., Lohmann, U., Raga, G. B., O'Dowd, C. D., Kulmala, M., Fuzzi, S., Reissell, A., Andreae, M. O.: Flood or drought: How do aerosols affect precipitation? Science, 321:1309-1313, 2008.

Rosenfeld, D., Sherwood, S., Wood, R., and Donner, L.: Climate effects of aerosol-cloud interactions. Science, 343: 379-380, 2014.

Rosenfeld, D., and Woodley, W. L.: Convective clouds with sustained highly supercooled liquid water down to _37_C, Nature, 405, 440–442, doi:10.1038/35013030, 2000.

Sassen, K., Starr, D., Mace, G. G., Poellot, M. R., Melfi, S. H., Eberhard, W.L., Spinhirne, J. D., Eloranta, E. W., Hagan, D. E., and Hallett, J.: The 5–6 December 1991 FIRE IFO II jet stream cirrus case study: Possible influences of volcanic aerosols, J. Atmos. Sci., 52, 97–123, doi:10.1175/1520-0469(1995) 052<0097:TDFIIJ>2.0.CO;2, 1995.

Shen, Y., Xiong, A., Wang, Y., and Xie, P.: Performance of high-resolution satellite precipitation products over China, J. Geophys. Res., 115, D02114, doi:10.1029/2009JD012097, 2010.

Sherwood, S.: Aerosols and ice particle size in tropical cumulonimbus, J. Clim., 15, 1051–1063, doi:10.1175/1520-0442(2002)015<1051:AAIPSI>2.0.CO;2, 2002.

Shinozuka, Y., Clarke, A. D., Nenes, A., Jefferson, A., Wood, R., McNaughton, C. S., Ström, J., Tunved, P., Redemann, J., Thornhill, K. L., Moore, R. H., Lathem, T. L., Lin, J. J., and Yoon, Y. J.: The relationship between cloud condensation nuclei (CCN) concentration and light extinction of dried particles: indications of underlying aerosol processes and implications for satellite-based CCN estimates, Atmos. Chem. Phys., 15, 7585-7604, 10.5194/acp-15-7585-2015, 2015.

Song, X. L. and Zhang, G. J.: Microphysics parameterization for connective clouds in a global climate model: Description and single-column model tests, J. Geophys. Res. Atmos., 116, D02201, 2011.

Squires, P.: The growth of cloud drops by condensation: I. general characteristics, Aust. J. Sci. Res., Ser. A, 5, 66–86, 1952.

Squires, P., and Twomey, S.: A comparison of cloud nucleus measurements over central North America and Caribbean Sea, J. Atmos. Sci., 23, 401–404, doi: 10.1175/1520-0469(1966)023<0401:ACOCNM> -2.0.CO;2, 1966.

Sun, Y. L., Wang, Z. F., Du, W., Zhang, Q., Wang, Q. Q., Fu, P. Q., Pan, X. L., Li, J., Jayne, J., and Worsnop, D. R.: Long-term real-time measurements of aerosol particle composition in Beijing, China: seasonal variations, meteorological effects, and source analysis, Atmos. Chem. Phys., 15: 10149-10165, 2015.

Tariq, S., and Ali, M.: Spatio-temporal distribution of absorbing aerosols over Pakistan retrieved form OMI on board Aura Satellite. Atmos. Pollution Res. doi: 10.5094/APR.2015.030, 2015.

Tao, M. H., Chen, L. F., Wang, Z. F., Tao, J. H., Che, H. Z., Wang, X. H., and Wang, Y.: Comparison and evaluation of the MODIS Collection 6 aerosol data in China. J. Geophys. Res. Atmos. 120:6992-7005, 2015.

Tao, W. K., Chen, J. P., Li, Z., Wang, C., and Zhang C.: Impact of aerosols on convective clouds and precipitation. Rev. Geophy., 50, RG2001/2012: 1-62, doi: 10.1029/2011RG000369, 2012.

Torres, O., Bhartia, P.K., Herman, J.R., Ahmad, Z., Gleason, J.: Derivation of aerosol properties from satellite measurements of backscattered ultraviolet radiation: Theoretical basis. J. Geophys. Res. Atmos. 103: 17099–17110, 1998.

Twohy, C. H., Coakley, J. A., and Tahnk, W. R.: Effect of changes in relative humidity on aerosol scattering near clouds, Journal of Geophysical Research: Atmospheres, 114, n/a-n/a, 10.1029/2008JD010991, 2009.

Twomey, S.: The influence of pollution on the shortwave albedo of clouds, J. Atmos. Sci., 34, 1149–1152, doi:10.1175/1520-0469(1977)034<1149:TIOPOT>2.0.CO;2, 1977.

Wang, J., Feng, J., Wu, Q., and Z. Yan, Z.: Impact of anthropogenic aerosols on summer precipitation in the Beijing-Tianjin-Hebei urban agglomeration in China: Regional climate modeling using WRF-Chem. Adv. Atmos. Sci., **33,** 753-766, 2016.

Wang, Z., Guo, P., and Zhang, H.: A Numerical Study of Direct Radiative Forcing Due to Black Carbon and Its Effects on the Summer Precipitation in China. Climatic and Environmental Research, **14,** 161-171, 2009.

Wolyn, P. G., and Mckee, T. B.: The mountain plains circulation east of a 2-km-high north south barrier,Mon. Weather Rev., 122, 1490-1508,1994.

Wu, P., Ding, Y. H., and Liu, Y. J.: Atmospheric circulation and dynamic mechanism for persistent haze events in the Beijing-Tianjin-Hebei region, Adv. Atmos. Sci.,34(4): 429-440, 2017.

Yang, X., Zhao, C., Zhou, L., Li, Z., Cribb, M., and Yang, S.: Wintertime cooling and a potential connection with transported aerosols in Hong Kong during recent decades. Atmos. Res. 211: 52-61, 2018.

Yu, R. C., Zhou, T. J., Xiong, A. Y., Zhu, Y. J., and Li, J. M.: Diurnal variations of summer precipitation over contiguous China. Geophys. Res. Lett. 34: L017041, 2007.

Yuan, T., Li, Z., Zhang, R., and Fan, J.: Increase of cloud droplet size with aerosol optical depth: An observation and modeling study. J. Geophys. Res. Atmos., 113: D04201, 2008.

Yuan, W. H., Yu, R. C., Chen, H. M., Li, J., and Zhang, M. H.: Subseasonal Characteristics of Diurnal Variation in Summer Monsoon Rainfall over Central Eastern China. J. Climate 23:6684-6695, 2010.

Zhou, S., Yang, J., Wang, W. C., Gong, D., Shi, P., and Gao, M.: Shift of daily rainfall peaks over the Beijing– Tianjin– Hebei region: An indication of pollutant effects? Int. J. Climatol. 2018:1–10. https://doi.org/10.1002/joc.5700, 2018.

Zeng, S., Riedi, J., Trepte, C. R., Winker, D. M., and Hu, Y. –X.: Study of global cloud droplet number concentration with A-Train satellites. Atmos. Chem. Phys., 14: 7125-7134, doi:

10.5194/acp-14-7125-2014, 2014.

Zhu, Y., Rosenfeld, D., and Li, Z.: Under what conditions can we trust retrieved cloud drop concentrations in broken marine stratocumulus? J. Geophys. Res. Atmos., 123: 8754-8767, 2018.

Tables

Indicator	Data from	Time	Clean/less (< 25th)	Polluted/more (>75th)
AOD	MODIS	2002-2012	0.98	2.00
CDNC (cm^{-3})	MODIS	2002-2012	699.20	2544.87
AAI	OMI	2005-2012	0.13	0.52
SAI	OMI	2005-2012	- 0.13	- 0.35
BC AOD	MACC	2003-2012	0.04	0.06
Sulfate AOD	MACC	2003-2012	0.46	0.87
Absolute humidity at 850 hPa (g/m^3)	ERA-interim	2002-2012	8.97	12.19

Table 1. The indicators used in the study and their thresholds for clean/less and polluted/more conditions.

Characteristics of heavy rainfall	Average of clean condition		Average of polluted condition		Difference (polluted - clean)		Significance of difference	
	AOD	CDNC	AOD	CDNC	AOD	CDNC	AOD	CDNC
Start time (LST)	**24.2**	**24.5**	**23.5**	**22.4**	**- 0.7**	**- 2.1**	**P<0.05**	**P<0.05**
Peak time (LST)	**23.0**	**23.1**	**22.0**	**18.9**	**- 1.0**	**- 4.2**	**P<0.05**	**P<0.05**
Duration (hours)	**4.0**	**4.9**	**4.8**	**7.3**	**+ 0.8**	**+ 2.4**	**P<0.05**	**P<0.05**
Intensity (0.1mm/hour)	**164.9**	**167.0**	**169.6**	**162.0**	**+ 4.7**	**- 5.0**	**P>0.1**	**P>0.1**

Table 2. The average values of start time (units: LST), peak time (units: LST), duration (units: hours) and intensity (units: 0.1mm/hour) of heavy rainfall respectively on clean condition and polluted condition using two indicators of AOD and CDNC, and the differences and significances of differences between clean and polluted conditions. "P<0.05" stands for the difference has passed the significance test of 95%, and "P>0.1" stands for the difference did not pass the significance test of 90%.

Group (case number)	CF	CTP	COT (liquid)	COT (ice)	CWP (liquid)	CWP (ice)	CER (liquid)	CER (ice)
1.Clean, dry (140)	67.9	460.3	4.9	4.1	62.5	80.4	21.1	34.6
2.Polluted, dry (75)	73.1 $0.05<p_{1,2}<0.1$	541.1	21.3	25.4	154.3	432.4	11.6	29.2
3.Clean, wet (191)	85.8	405.1	6.3	7.4	79.3	150.8	20.3 $0.05<p_{1,3}<0.1$	34.7 $p_{1,3}>0.1$
4.Polluted, wet (338)	97.5	414.2 $p_{3,4}>0.1$	41.2	31.0 $0.05<p_{2,4}<0.1$	351.2	523.7 $p_{2,4}>0.1$	13.0	25.5

Table 3. The average values of CF (units: %), CTP (units: hPa), COT (liquid and ice, units: none), CWP (liquid and ice, units: g/m^2) and CER (liquid and ice, units: μm) in four groups. Grey numbers represent the differences are not significant, in which "0.05<P<0.1" stands for the difference has passed the significance test of 90% but did not pass the significance test of 95%, and "P>0.1" stands for the difference did not pass the significance test of 90%.

Figures

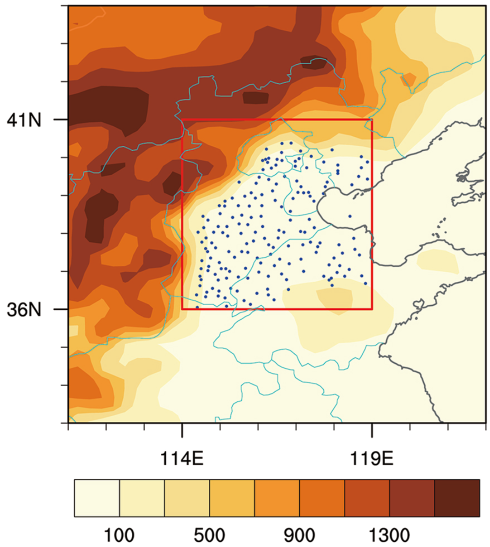

Figure 1. Altitudes (shading, units: m) and selected stations (dots) in the BTH region (red box, 36–41° N, 114–119° E).

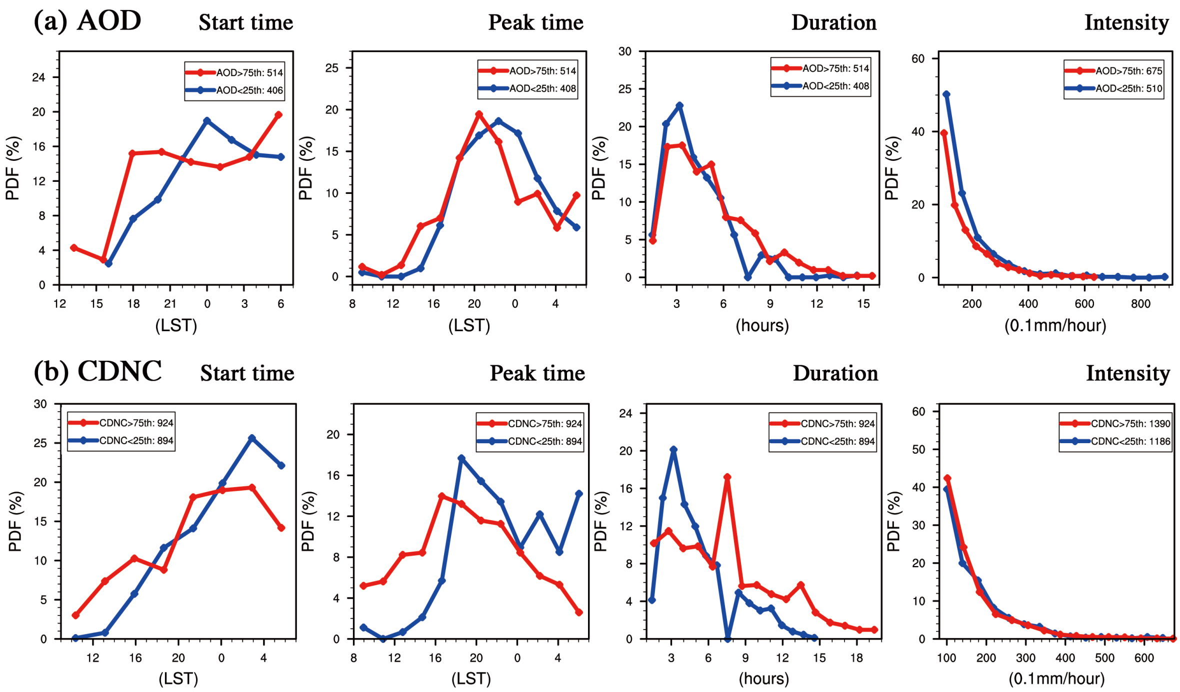

Figure 2. PDF of start time (units: LST), peak time (units: LST), duration (units: hours) and intensity (units: 0.1mm/hour) of heavy rainfall on selected clean (blue lines) and polluted (red lines) conditions, respectively using indicator of (a) AOD and (b) CDNC (cm^{-3}), during early summers from 2002 to 2012.

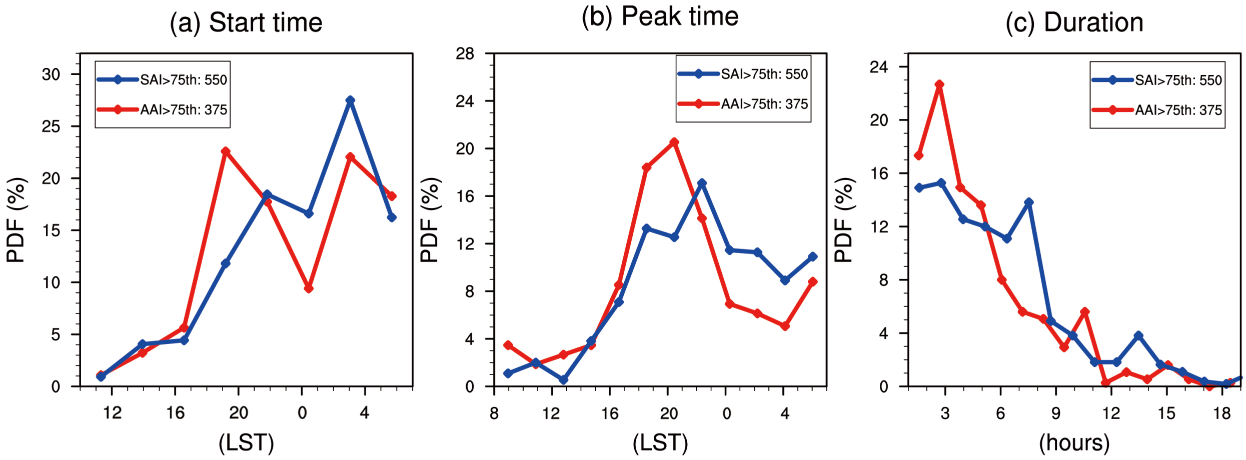

Figure 3. PDF of (a) start time (units: LST), (b) peak time (units: LST), and (c) duration (units: hours) of heavy rainfall on the days that SAI more than 75th percentile (blue lines) and days that AAI more than 75th percentile (red lines), during early summers from 2005 to 2012. The differences between two groups have all passed the significant test of 95%.

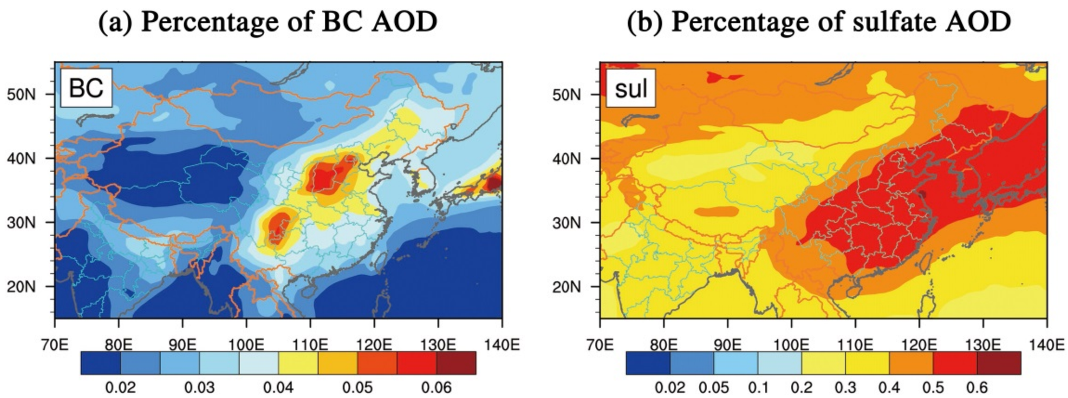

Figure 4. Percentages of AOD for (a) BC and (b) sulfate in JJA during 2002 to 2012.

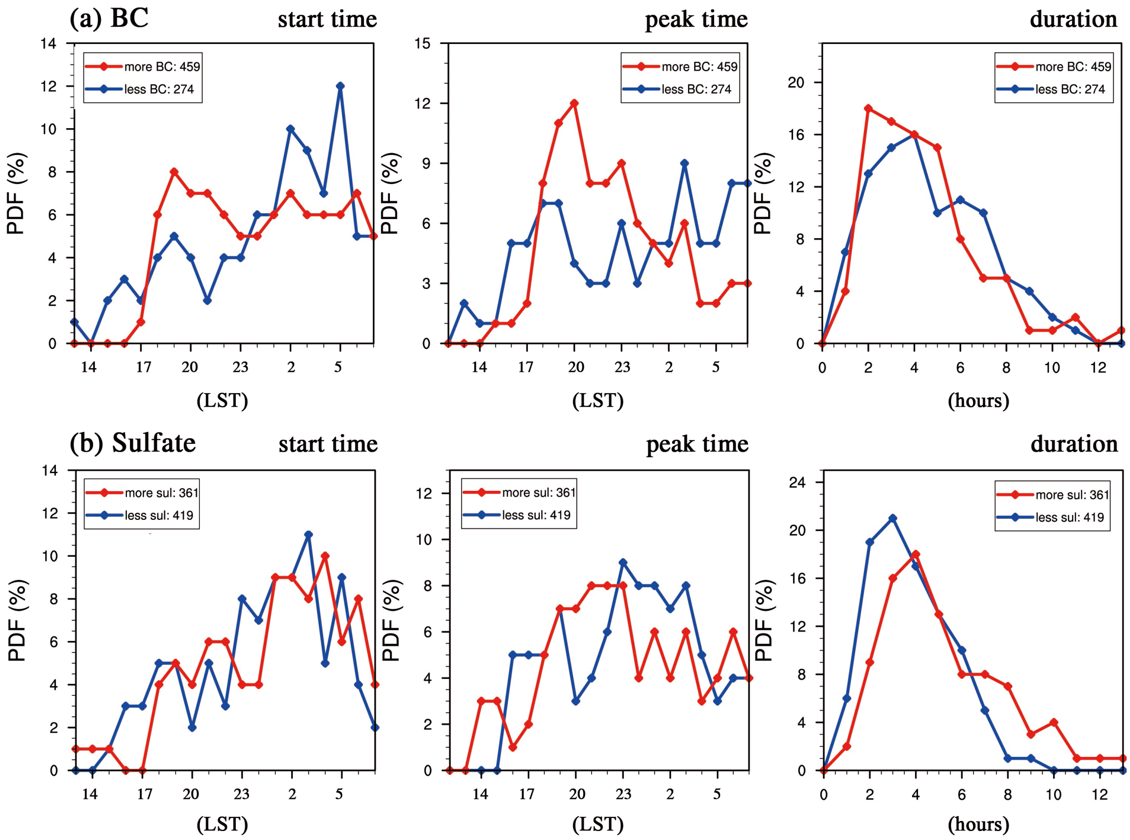

Figure 5. PDF of start time (units: LST), peak time (units: LST) and duration (units: hours) of heavy rainfall in different conditions of (a) BC and (b) sulfate. Blue/red lines stand for the condition of less/more BC or sulfate during early summers from 2003 to 2012. The differences have passed the significant test of 95%.

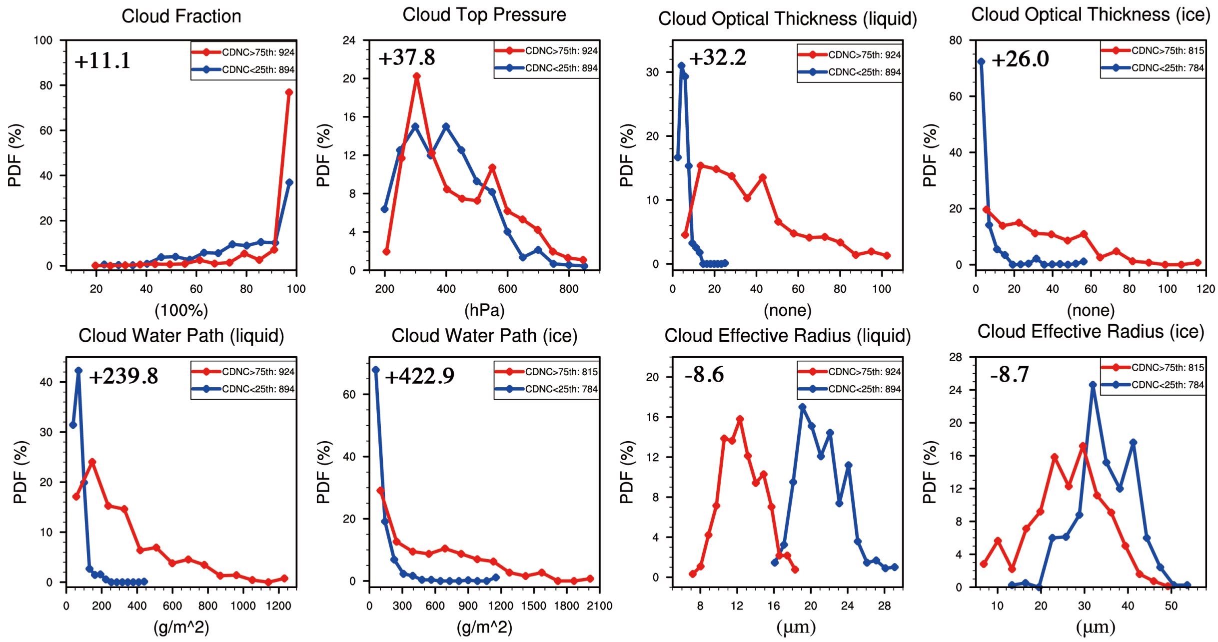

Figure 6. PDF of CF (units: %), CTP (units: hPa), COT (liquid and ice, units: none), CWP (liquid and ice, units: g/m^2) and CER (liquid and ice, units: μm) on selected clean (blue lines: CDNC<25th percentile) and polluted (red lines: CDNC>75th percentile) heavy rainfall days. The numbers in the upper left stand for the mean differences between polluted and clean days (polluted minus clean). The differences between clean and polluted cases have all passed the significant test of 95%.

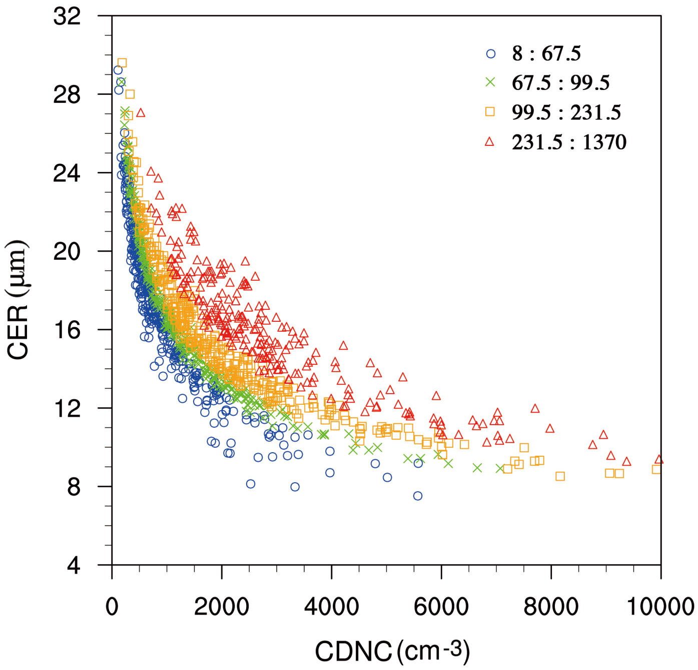

Figure 7. Relationship of CER (units: μm) and CDNC (cm^{-3}) on different conditions of CWP (units: g/m^2). Different colors stand for different CWP conditions as shown in the legend.

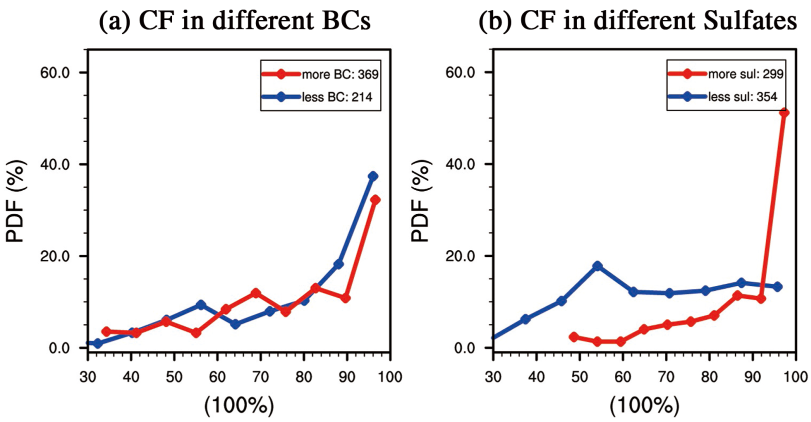

Figure 8. PDF of CF (units: 100%) respectively for selected less BC/sulfate (blue lines) and more BC/sulfate (red lines) cases with heavy rainfall during 10 early summers (2003-2012).

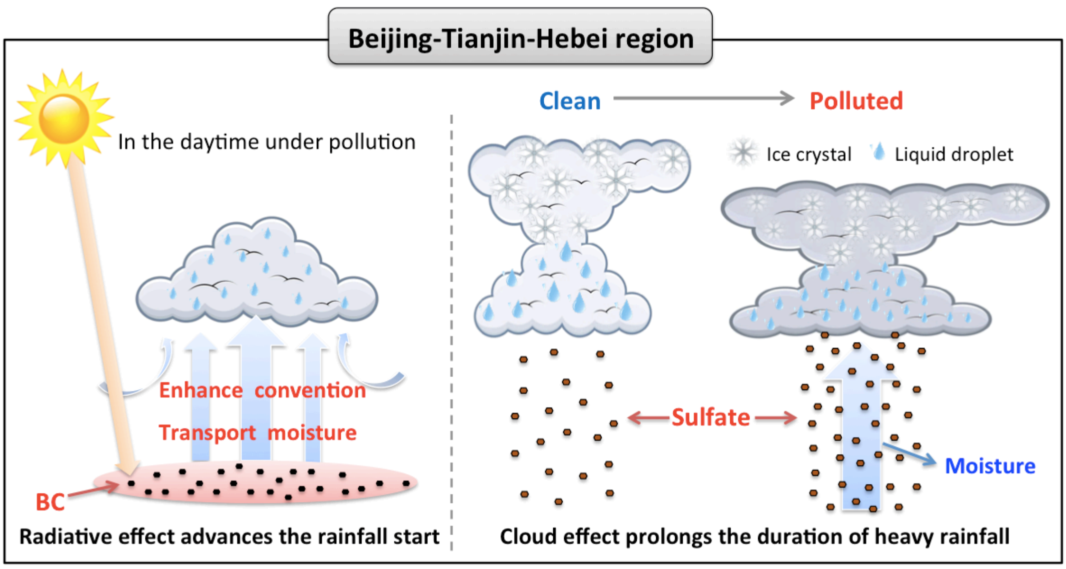

Figure 9. A schematic diagram for aerosols impact on heavy rainfall over Beijing-Tianjin-Hebei region.